

Erbin interacts with TARP γ -2 for surface expression of AMPA receptors in cortical interneurons

Yanmei Tao^{1,2,7}, Yong-Jun Chen^{2,7}, Chengyong Shen^{2,7}, Zhengyi Luo⁴, C Ryan Bates², Daehoon Lee², Sylvie Marchetto⁵, Tian-Ming Gao⁴, Jean-Paul Borg⁵, Wen-Cheng Xiong^{2,6} & Lin Mei^{2-4,6}

Inhibitory neurons control the firing of glutamatergic neurons and synchronize brain activity. However, little is known about mechanisms of excitatory synapse formation in inhibitory neurons. Here we demonstrate that Erbin is specifically expressed in cortical inhibitory neurons. It localizes at excitatory synapses and regulates AMPA receptor (AMPA) surface expression. Erbin mutation reduced mEPSCs and AMPAR currents specifically in parvalbumin (PV)-positive interneurons but not in pyramidal neurons. We found that the AMPAR auxiliary protein TARP γ -2 was specifically expressed in cortical interneurons. Erbin interacts with TARP γ -2 and is crucial for its stability. Deletion of the γ -2-interacting domain in Erbin attenuated surface AMPAR and excitatory transmission in PV-positive interneurons. Furthermore, we observed behavioral deficits in Erbin-null mice and in mice expressing an Erbin truncation mutant that is unable to interact with TARP γ -2. These observations demonstrate a crucial function for Erbin in AMPAR surface expression in cortical PV-positive interneurons and may contribute to a better understanding of psychiatric disorders.

GABAergic interneurons shape the responses of pyramidal neurons and control the timing of their excitation and thus refine cortical receptive fields, and they generate—as well as pace—synchronous oscillatory activities of population of neurons¹. They are crucial for interactions between cortical networks to ensure sophisticated motor, sensory and cognitive function^{1,2}. Dysfunction of interneurons, and PV-positive interneurons in particular, has been implicated in psychiatric disorders including schizophrenia and autism^{3,4}. The activity of GABAergic interneurons is regulated by excitatory and inhibitory neurons^{2,5}. Unlike excitatory synapses on pyramidal neurons, in which axon terminals synapse on protruded spines, glutamatergic synapses on interneurons are on dendritic shafts^{1,2}. Moreover, synaptic plasticity in interneurons can be regulated by calcium-permeable AMPARs that do not contain the GluA2 subunit⁶. Excitatory synapses in excitatory neurons have been studied extensively; however, little is known about the mechanisms underlying excitatory synapse formation on interneurons.

Surface expression and trafficking of AMPARs is regulated by interacting proteins including TARPs (transmembrane AMPAR regulatory proteins), protein interacting with C kinase 1 (PICK1), synapse-associated protein 97 (SAP97), glutamate receptor-interacting protein (GRIP), *N*-ethylmaleimide-sensitive fusion protein (NSF) and protein 4.1N (refs. 7,8). In particular, TARPs are considered auxiliary subunits of AMPARs, and they are necessary for sensitivity to glutamatergic agonists and antagonists and channel desensitization, in addition to surface expression and synaptic trafficking^{7,9,10}. TARPs have several

isoforms that are expressed in different neurons of different brain regions⁹⁻¹². TARP γ -2 (or γ -2, also called stargazin), the first TARP family member identified from the spontaneous-mutant mouse line stargazer, regulates AMPAR in cerebellar granule cells and stellate cells¹³⁻¹⁶. Evidence indicates that TARPs γ -2 and γ -3 work in Golgi cells¹⁷, γ -2 and γ -7 in Purkinje cells^{17,18}, γ -4 and γ -5 in Bergmann glial cells^{11,12,19} and γ -2 and γ -8 in hippocampal pyramidal and inhibitory neurons^{10,20,21}. *In situ* studies reveal high levels of γ -3 and lower expression of γ -2, γ -4 and γ -8 in neocortex^{11,12}; however, less is known about TARP function in cortical neurons, especially cortical interneurons, because both synaptic and extrasynaptic AMPAR currents are normal in cortical plate neurons carrying mutant forms of γ -2, γ -3 and γ -4 (ref. 10). Moreover, little is known about how TARP expression is regulated.

Erbin is an adaptor protein that contains leucine-rich repeats (LRRs) at the N terminus, a PDZ domain at the C terminus and a large nonconserved domain in between^{22,23}. It interacts with various proteins, including postsynaptic density protein 95 (PSD95)²³, a postsynaptic scaffold protein of excitatory synapses, and has been implicated in regulating the assembly of adherence junctions and signaling pathways of neuregulin, Ras and transforming growth factor- β ^{22,24-27}. Here, we provide evidence that Erbin is specifically expressed in GABAergic interneurons in the neocortex and hippocampus and localized at excitatory synapses of interneurons. In mice, ablation of the gene encoding Erbin (*Erbp2ip*, also known as *erbin*), reduced AMPAR surface levels and impaired the glutamatergic transmission

¹Institute of Developmental and Regenerative Biology, College of Life and Environmental Sciences, Hangzhou Normal University, Hangzhou, Zhejiang, China. ²Institute of Molecular Medicine and Genetics, Medical College of Georgia, Georgia Regents University, Augusta, Georgia, USA. ³Department of Neurology, Medical College of Georgia, Georgia Regents University, Augusta, Georgia, USA. ⁴Department of Neurobiology, Southern Medical University, Guangzhou, China. ⁵CRCM, Inserm, U1068; Institut Paoli-Calmettes; Aix-Marseille Université; CNRS, UMR 7258, Marseille, France. ⁶Charlie Norwood VA Medical Center, Augusta, Georgia, USA. ⁷These authors contributed equally to this work. Correspondence should be addressed to L.M. (lmei@gru.edu).

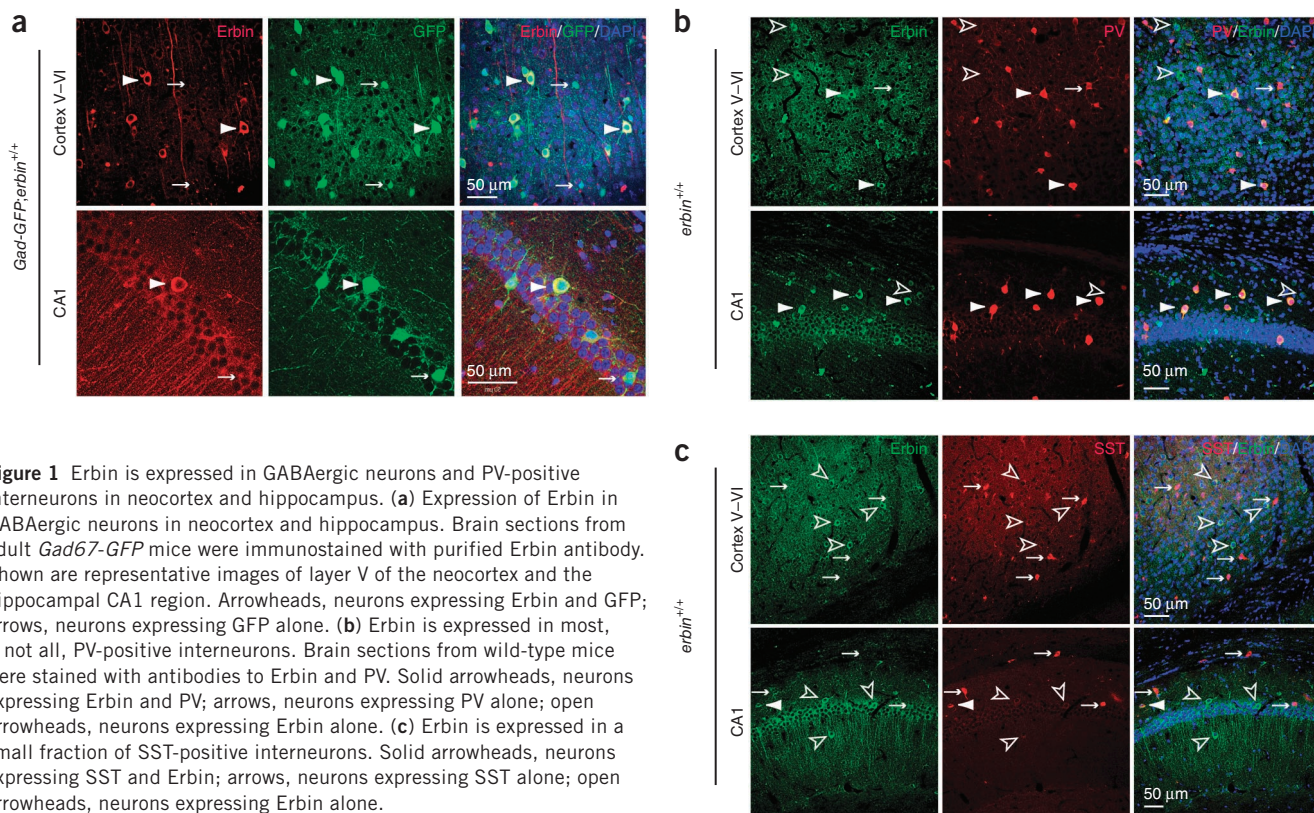


Figure 1 Erbin is expressed in GABAergic neurons and PV-positive interneurons in neocortex and hippocampus. **(a)** Expression of Erbin in GABAergic neurons in neocortex and hippocampus. Brain sections from adult *Gad67-GFP* mice were immunostained with purified Erbin antibody. Shown are representative images of layer V of the neocortex and the hippocampal CA1 region. Arrowheads, neurons expressing Erbin and GFP; arrows, neurons expressing GFP alone. **(b)** Erbin is expressed in most, if not all, PV-positive interneurons. Brain sections from wild-type mice were stained with antibodies to Erbin and PV. Solid arrowheads, neurons expressing Erbin and PV; arrows, neurons expressing PV alone; open arrowheads, neurons expressing Erbin alone. **(c)** Erbin is expressed in a small fraction of SST-positive interneurons. Solid arrowheads, neurons expressing SST and Erbin; arrows, neurons expressing SST alone; open arrowheads, neurons expressing Erbin alone.

onto interneurons, indicating that Erbin has a function in excitatory synapses of interneurons. Further studies indicate that this effect requires interaction with TARP γ -2. We explored Erbin's molecular mechanisms and studied *erbin* ^{Δ C/ Δ C} mice, which express an Erbin truncation mutant that is unable to interact with TARP γ -2. Both Erbin-null (*erbin*^{-/-}) and *erbin* ^{Δ C/ Δ C} mice have similar behavioral deficits associated with brain disorders. These observations indicate that Erbin is necessary for surface expression of AMPARs in interneurons through control of TARP γ -2 levels, identifying a previously unknown regulatory mechanism of synaptic transmission.

RESULTS

Erbin is expressed in GABAergic interneurons

To determine which neurons express Erbin, we generated an antibody to Erbin (anti-Erbin) called E2/E2 by immunizing rabbits with a fusion protein consisting of the Erbin middle domain (amino acids (aa) 465–818) and glutathione *S*-transferase (GST). E2/E2 recognized a single protein at the predicted size (180 kDa) in western blots of brain homogenates (**Supplementary Fig. 1a**). The immunoreactivity was abolished in samples from *erbin*^{-/-} mice, indicating high specificity of the antibody (**Supplementary Fig. 1a**). Immunostaining with the E2/E2 antibody revealed that Erbin-immunoreactive cells were scattered in layers II–VI in the cortex and in CA1, CA2, CA3 and dentate gyrus of the hippocampus (**Supplementary Fig. 1b,c**). Again, the signal was abolished in slices from *erbin*^{-/-} mice (**Supplementary Fig. 1b**). The pattern of distribution suggested that Erbin may be present in GABAergic interneurons.

To test this hypothesis, we isolated brain slices from *Gad67-GFP* mice, which express GFP under the control of the promoter of *Gad67* (encoding GABA-synthesizing enzyme glutamic acid decarboxylase 67), in GABAergic neurons²⁸. Erbin was present in GFP-expressing neurons and not in cells lacking GFP (**Fig. 1a**). GABAergic interneurons

are heterogeneous in function, morphology and expression of distinct markers^{1,2}. We found that, $71.6 \pm 4.3\%$ (mean \pm s.d.) of GFP-positive neurons in cortex and $60.3 \pm 6.1\%$ in hippocampus were labeled by the E2/E2 antibody, suggesting that Erbin is expressed in select interneurons.

PV-positive and somatostatin (SST)-positive interneurons are two major GABAergic interneurons, accounting for 40–50% and 16–30%, respectively, of cortical interneurons^{28–30}. PV is a marker of basket and chandelier cells that form perisomatic and axo-axonal synapses on pyramidal neurons, whereas SST is expressed mainly in Martinotti cells that innervate distal dendrites of pyramidal neurons⁵. To determine which type of GABAergic neuron expresses Erbin, we stained slices with E2/E2 and antibodies to PV or SST. Almost all PV-positive neurons in the cortex and hippocampus ($94.8 \pm 3.2\%$ and $89.3 \pm 8.3\%$, respectively) were labeled by the anti-Erbin antibody (**Fig. 1b**). Of the Erbin-positive neurons in the cortex and hippocampus, $81.1 \pm 5.2\%$ and $83.1 \pm 3.7\%$ expressed PV, respectively, and $2.4 \pm 2.2\%$ and $20.2 \pm 3.0\%$ were co-stained with the antibody to SST (**Fig. 1c**). These results indicate that Erbin is specifically expressed in interneurons, mainly PV-positive interneurons in the neocortex and hippocampus.

Erbin deficiency causes behavioral deficits

Dysfunction of GABAergic interneurons, particularly PV-positive interneurons, is implicated in the pathophysiology of a growing number of psychiatric disorders^{4,31–33}. Deficits in PV-positive interneurons in rodents have been associated with abnormal locomotive behavior and impaired prepulse inhibition (PPI), indicating a deficiency in basic sensorimotor function^{31,32}. To investigate the function of Erbin, we determined whether Erbin-null mice exhibited any behavioral abnormality associated with interneuron deficits. We observed increases in ambulatory count and travel distance in *erbin*^{-/-} mice as compared to control wild-type (*erbin*^{+/+}) littermates within 30 min in the

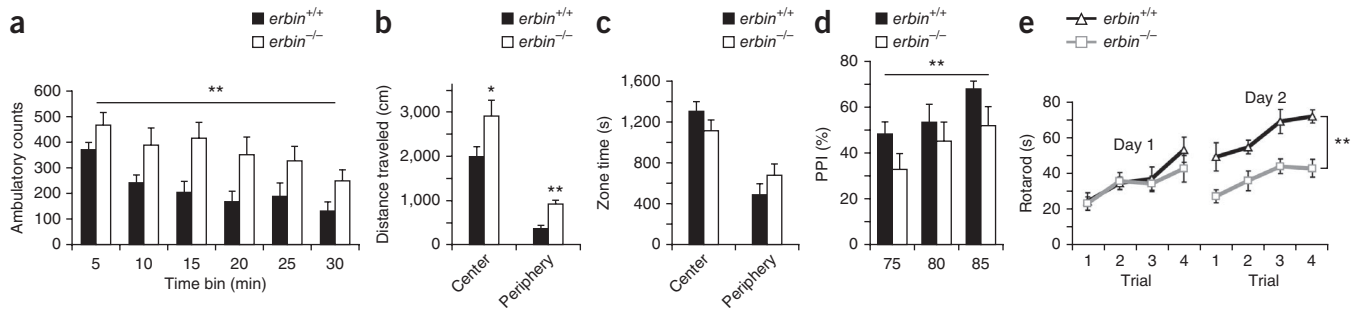


Figure 2 Behavioral deficits in Erbin-null mice as compared to wild-type controls. **(a)** Ambulatory counts for *erbin*^{+/+} and *erbin*^{-/-} mice in open-field tests. Error bars, mean \pm s.e.m.; $**P < 0.0001$, $F_{1,17} = 8.607$, two-way analysis of variance (ANOVA). **(b)** Increased travel distance by *erbin*^{-/-} mice in central and peripheral areas in open-field tests. Error bars, mean \pm s.e.m.; $*P = 0.0236$, $t_{17} = 2.139$ for center data, $**P < 0.0001$, $t_{17} = 4.811$ for periphery data, unpaired *t* test. **(c)** *erbin*^{-/-} and *erbin*^{+/+} mice spent similar amounts of time in central and peripheral areas. Error bars, mean \pm s.e.m.; $P = 0.1106$, $t_{17} = 1.270$ for center and periphery data, unpaired *t* test. **(d)** PPI in *erbin*^{-/-} and *erbin*^{+/+} mice. Error bars, mean \pm s.e.m.; $**P = 0.0082$, $F_{1,17} = 2.788$, two-way ANOVA. **(e)** Latency to fall from accelerating rotarod in second-day trials. Error bars, mean \pm s.e.m.; $**P < 0.0001$, $F_{1,17} = 5.608$, two-way ANOVA. For **a–e**, $n = 9$ *erbin*^{+/+} mice or 10 *erbin*^{-/-} mice.

open-field tests (**Fig. 2a,b**). We observed no difference in the amount of time spent in the central area (**Fig. 2c**), indicating that *erbin*^{-/-} mice may not have anxiety-related behaviors, and we saw no differences in stereotypic count and vertical count (data not shown), suggesting that *erbin*^{-/-} mice had normal exploratory activity. To evaluate the PPI of *erbin*^{-/-} mice, we used a combination of an auditory-evoked startle stimulus (120 dB) and three levels of prepulse stimuli (75, 80 and 85 dB). *erbin*^{-/-} mice showed startle responses similar to those of wild-type littermates, indicating normal hearing and acoustic startle reflex. However, PPI was substantially lower in Erbin-null mice than in littermate controls (**Fig. 2d**). These results suggest impairment in forebrain neural circuits and sensory gating. In addition, *erbin*^{-/-} mice were deficient in motor coordination, as indicated by poor performance in rotarod tests (**Fig. 2e**). This deficit

did not seem to be caused by deficits in peripheral nerves or motor reflex, because *erbin*^{-/-} mice showed a slight increase in grip strength as compared to controls ($P = 0.0017$, $t_{17} = 3.399$, unpaired *t* test).

Erbin regulates excitatory transmission in interneurons

Next, we examined the subcellular location of Erbin. We stained dissociated cortical or hippocampal neurons with the E2/E2 antibody

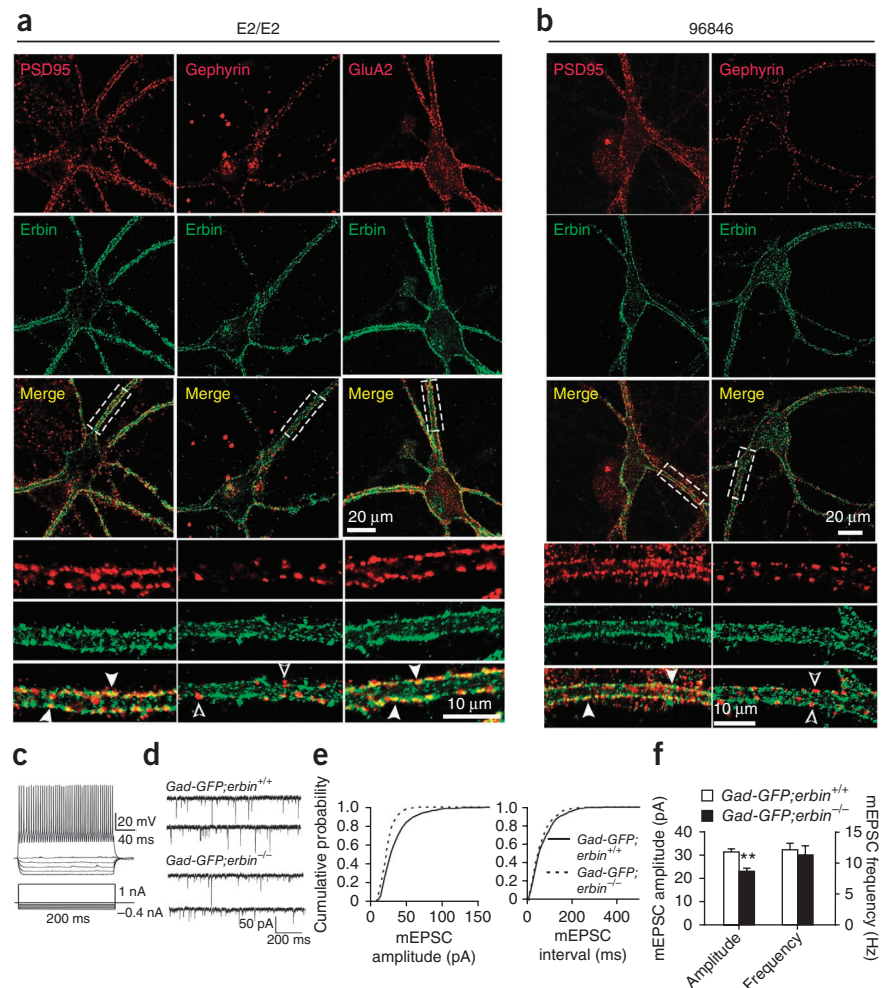


Figure 3 Erbin is required for excitatory synaptic transmission of PV-positive inhibitory neurons. **(a,b)** Erbin was localized at excitatory synapses. DIV 21 neurons at low density were stained with anti-Erbin antibodies E2/E2 (**a**) and 96846 (**b**) and postsynaptic markers (PSD95, gephyrin or GluA2). Solid arrowheads, double-positive puncta; open arrowheads, puncta positive for gephyrin only. **(c)** Nonadaptive firing pattern of fast-spiking interneurons. Fast-spiking interneurons were identified on the basis of characteristic membrane and fast-spiking properties from GFP-positive cells. Hyperpolarizing and depolarizing current steps were applied for 200 ms at 0.2 Hz in current-clamp configuration. **(d)** Representative traces of mEPSCs in fast-spiking interneurons in *erbin*^{-/-} and control littermates. **(e)** Cumulative distributions of mEPSC amplitudes and inter-event intervals of data in **d**. **(f)** Reduced amplitudes, but not frequencies, of mEPSCs in *erbin*^{-/-} PV-positive interneurons. $n = 12$ cells from six *erbin*^{+/+} mice or 11 cells from six *erbin*^{-/-} mice. Error bars, mean \pm s.e.m.; $**P = 0.004$, $t = 3.187$ for amplitude; $P = 0.733$, $t = 0.345$ for frequency, unpaired *t* test.

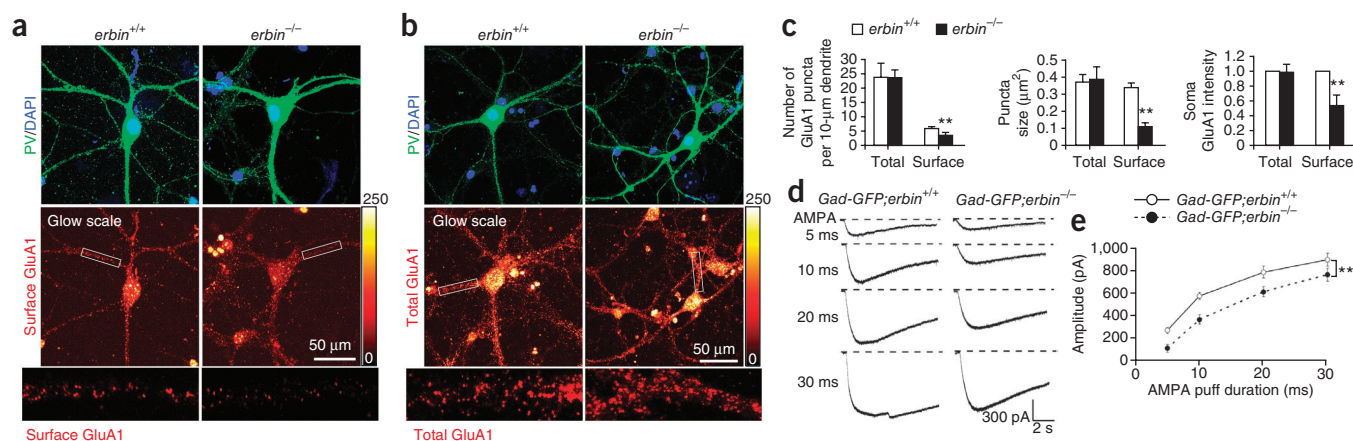


Figure 4 Reduced AMPAR surface expression in *erb1^{-/-}* PV-positive interneurons. **(a)** Surface AMPAR levels were reduced in *erb1^{-/-}* PV-positive interneurons. DIV 17 cortical neurons were stained with an anti-N-terminal GluA1 antibody under non-permeabilizing conditions then permeabilized and stained with an anti-PV antibody. GluA1 staining intensity in primary dendrites and soma was quantified. Side bar, glow scale of GluA1 staining intensity (arbitrary unit). **(b)** Total AMPAR levels were not changed in *erb1^{-/-}* PV-positive interneurons. DIV 17 cortical neurons were permeabilized and stained with anti-N-terminal GluA1 and anti-PV antibodies. GluA1 staining intensity in primary dendrites and soma was quantified. Side bar, glow scale of GluA1 staining intensity. **(c)** Quantitative analysis of data in **a** and **b**. $n = 20$ cells (for *erb1^{+/+}* cultures) or 15 cells (for *erb1^{-/-}* cultures) from three independent experiments. Error bars, mean \pm s.d.; $**P = 0.0026$, $t = 4.292$ for puncta number; $**P = 0.0020$, $t = 10.88$ for puncta size; $**P = 0.0020$, $t = 8.066$ for soma GluA1 intensity; unpaired t test. **(d)** AMPA-evoked inward currents in *erb1^{-/-}* PV-positive interneurons. Shown are representative current traces of GFP-positive, fast-spiking interneurons from indicated genotypes, clamped at -70 mV. AMPA ($500 \mu\text{M}$) was locally applied to soma using air pressure for various durations (6 p.s.i., 5–30 ms). **(e)** Quantitative analysis of peak currents as in **d**. $n = 9$ cells from three *erb1^{-/-}* mice or 8 cells from three *erb1^{+/+}* mice; error bars, mean \pm s.e.m.; $**P < 0.0001$, $F = 28.51$, two-way ANOVA.

and markers of excitatory or inhibitory synapses. As in the brain slices, Erbin was detectable in some, but not all, neurons that were positive for GAD65, another synthase of GABA (Supplementary Fig. 2a), in agreement with the notion that Erbin is expressed in select GABAergic neurons. Notably, Erbin was enriched in puncta in dendritic shafts of interneurons (Supplementary Fig. 2b), suggesting localization in postsynaptic compartments. We observed PSD95 co-staining in $88.2 \pm 2.3\%$ of Erbin-positive puncta (Fig. 3a), indicating that the majority of Erbin puncta are localized at excitatory synapses. To test this idea further, we used the anti-Erbin antibody 96846, which was raised against a different epitope—the C-terminal region of Erbin (aa 1241–1371) containing the PDZ domain²³. Staining with affinity-purified 96846 revealed that $83.3 \pm 5.7\%$ of Erbin puncta were positive for PSD95 (Fig. 3b), in agreement with results obtained with the E2/E2 antibody. We then co-stained neurons with E2/E2 or 96846 and an antibody to vGluT, a presynaptic marker of excitatory synapses. vGluT-positive puncta were partially superposed with those of Erbin along the dendritic shafts identified by E2/E2 or 96846 (Supplementary Fig. 3a). We also detected Erbin in $88.6 \pm 4.4\%$ of puncta that were labeled with the AMPAR subunit GluA2 (Fig. 3a). Finally, and in contrast, only a few Erbin-positive puncta co-stained with markers of inhibitory synapses such as gephyrin or vGAT (Fig. 3a,b and Supplementary Fig. 3a). Together, these observations suggest that Erbin is localized in the postsynaptic compartments of excitatory synapses in GABAergic neurons. A fraction of Erbin-positive puncta, revealed by E2/E2 or 96846, did not colocalize with PSD95 (Fig. 3a,b). They appeared to be inside dendrites and soma and positive for EEA1, a marker of early endosomes, suggesting that they may represent Erbin in early endosomes (Supplementary Fig. 3b).

To investigate the function of Erbin at excitatory synapses of interneurons, we characterized *erb1^{-/-}* mice. They showed similar laminar cortical structures, hippocampal structures and numbers of total neurons in the cortex to those of controls (Supplementary Fig. 4a and data not shown). We observed no difference between the

genotypes in the number of PV-positive neurons and their location, soma size and primary dendrite number in the cortex (Supplementary Fig. 4a–d). These observations suggest that Erbin mutation has little effect on cortical lamination and development of pyramidal and PV-positive neurons. To identify interneurons for electrophysiological recording, we crossed *erb1^{-/-}* mice with *Gad67-GFP* mice to generate *Gad-GFP;erb1^{-/-}* mice, in which interneurons could be identified by GFP expression²⁸. Because Erbin was expressed mainly in PV-positive neurons, we focused on neurons that showed characteristic firing properties—nonadapting repetitive firing of fast spikes after depolarizing current injections⁵ (Fig. 3c). To ensure that recorded fast-spiking interneurons were indeed PV positive, we injected them with biocytin. We observed co-staining of biocytin and PV in recorded neurons, indicating successful identification of PV-positive neurons for recording (Supplementary Fig. 5a). Erbin deficiency had no effect on resting membrane potentials, input resistance and time constant or depolarization-triggered spiking (amplitudes, thresholds, frequencies and after-hyperpolarization (AHP) amplitudes) of fast-spiking interneurons (Supplementary Table 1).

We analyzed spontaneous miniature excitatory postsynaptic currents (mEPSCs) in PV-positive interneurons in prefrontal cortical slices in the presence of tetrodotoxin (TTX, $1 \mu\text{M}$) and bicuculline methiodide (BMI, $20 \mu\text{M}$). The mEPSCs recorded under these conditions were inhibited by CNQX, an AMPAR antagonist, suggesting that they were mediated by AMPAR (data not shown). The mEPSCs of PV-positive interneurons had lower amplitudes in *erb1^{-/-}* mice than in controls (Fig. 3d–f). In contrast, mEPSC amplitudes and frequencies in pyramidal neurons, which were GFP-negative and had adapting firing of spikes after depolarizing current injections, did not differ between *erb1^{-/-}* mice and controls (Supplementary Fig. 5b–e). These results demonstrate that Erbin mutation impairs AMPAR-mediated synaptic transmission specifically in PV-positive interneurons but not pyramidal neurons. The lack of alteration in mEPSC frequency in PV-positive interneurons suggests that Erbin deficiency has no effect on glutamate release at excitatory synapses.

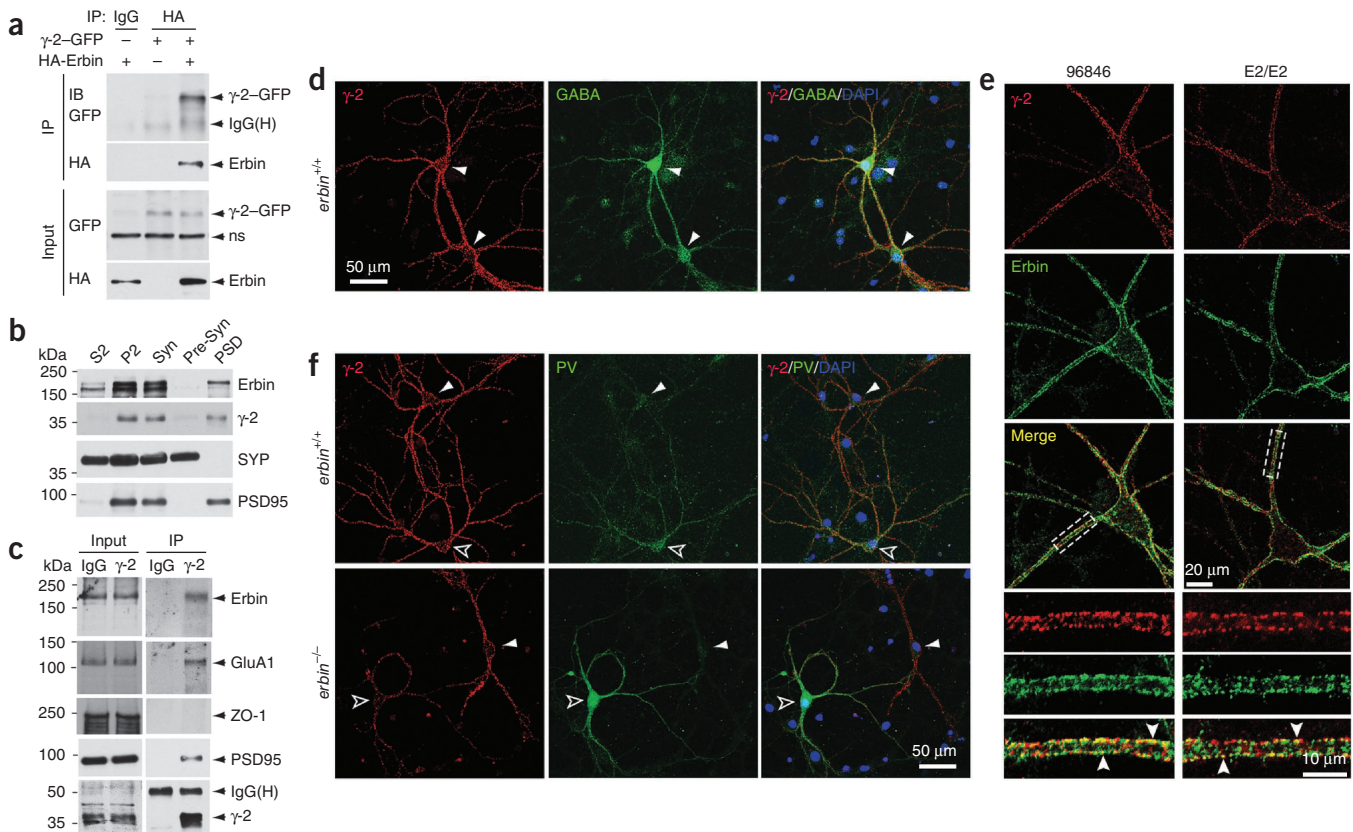


Figure 5 Erbin interaction with γ -2 and regulation of its expression. **(a)** Erbin interaction with γ -2 in HEK293 cells transfected with γ -2-GFP without or with hemagglutinin-tagged Erbin (HA-Erbin). Lysates were incubated with anti-HA antibody, and precipitates were blotted with anti-GFP antibody. Lysates were blotted directly to indicate input. IgG(H), IgG heavy chain. ns, nonspecific band; IB, immunoblot. **(b)** Co-purification of γ -2 and Erbin in PSD fractions of the cortex. Mouse cortices were fractionated as described in Online Methods and blotted for indicated proteins. Syn, synaptosome; pre-Syn, pre-synaptic fraction; SYP, synaptophysin. P2, pellet 2; S2, supernatant 2. **(c)** Erbin association with γ -2 *in vivo*. Cortical S1 fractions were prepared as described in Online Methods and incubated with anti- γ -2 antibody or regular rabbit IgG (as control). Precipitates were probed with antibodies to the proteins indicated. Cortical S1 fractions were blotted directly to indicate input. **(d)** Expression of γ -2 in GABAergic neurons. Cortical neurons were stained with mouse monoclonal anti- γ -2 and rabbit polyclonal anti-GABA antibodies, which were visualized by Alexa 594- and Alexa 488-labeled secondary antibodies, respectively. Arrowheads, GABAergic neurons. **(e)** Colocalization of γ -2 and Erbin in cortical interneurons. Cortical cultures were stained with mouse anti- γ -2 and rabbit anti-Erbin (E2/E2 or 96846, respectively) antibodies. **(f)** γ -2 in PV-positive interneurons from *erbin*^{-/-} and *erbin*^{+/+} mice. Cortical neurons were probed with mouse monoclonal anti- γ -2 and rabbit polyclonal anti-PV antibodies, which were visualized by Alexa 594- and Alexa 488-labeled secondary antibodies, respectively. Open arrowheads, PV-positive interneurons; solid arrowheads, PV-negative GABAergic neurons. Full-length blots are presented in **Supplementary Figure 11**.

In support of this hypothesis were observations that paired-pulse ratios of evoked EPSCs were not changed in interneurons of *erbin*^{-/-} mice (**Supplementary Fig. 6a–d**).

To test whether Erbin deficiency changes transmission mediated by NMDARs (*N*-methyl-D-aspartate receptors), we measured NMDAR-mediated mEPSCs of fast-spiking interneurons by blocking both AMPARs (CNQX, 20 μ M) and GABA_A channels (BMI, 20 μ M). Consistent with previous reports³⁴, about two-thirds of fast-spiking interneurons exhibited NMDAR-mediated mEPSCs (NMDAR-mEPSCs) (**Supplementary Fig. 6e–g**), which were abolished by the NMDAR blocker DL-AP5. There was no significant difference in amplitudes, frequencies and decay times of NMDAR-mEPSCs of fast-spiking interneurons between *erbin*^{-/-} and *erbin*^{+/+} mice (**Supplementary Fig. 6g**). These results indicate that Erbin does not regulate NMDAR-mediated synaptic transmission in fast-spiking interneurons. Moreover, amplitudes and frequencies of miniature inhibitory postsynaptic currents (mIPSCs) recorded in fast-spiking interneurons were similar in *erbin*^{-/-} mice and *erbin*^{+/+} littermates (**Supplementary Fig. 6h,i**), suggesting little effect of Erbin deficiency

on inhibitory synaptic transmission on fast-spiking interneurons. This result is consistent with the observation that Erbin did not associate with inhibitory synaptic proteins (**Fig. 3a,b**). Together, these observations demonstrate that Erbin deficiency specifically impairs AMPAR-mediated currents in PV-positive interneurons.

Erbin regulates surface expression of AMPARs

To understand mechanisms of AMPAR current impairment by Erbin deficiency, we first determined whether it alters channel properties of AMPARs. A majority (78%) of fast-spiking interneurons in prefrontal cortex contain mostly calcium-permeable (GluA2-lacking) AMPARs that are fast gating and can be blocked in a voltage-dependent manner by intracellular polyamines and, thus, show inwardly rectifying current-voltage (*I*-*V*) curves³⁵. The rise and decay times of mEPSCs in fast-spiking interneurons in which Erbin is enriched were similar between wild-type and *erbin*^{-/-} mice (**Supplementary Fig. 7a,b**), suggesting that Erbin deficiency may not alter synaptic AMPAR gating. Moreover, we observed no difference between wild-type and *erbin*^{-/-} fast-spiking interneurons in the rectification index recorded in the

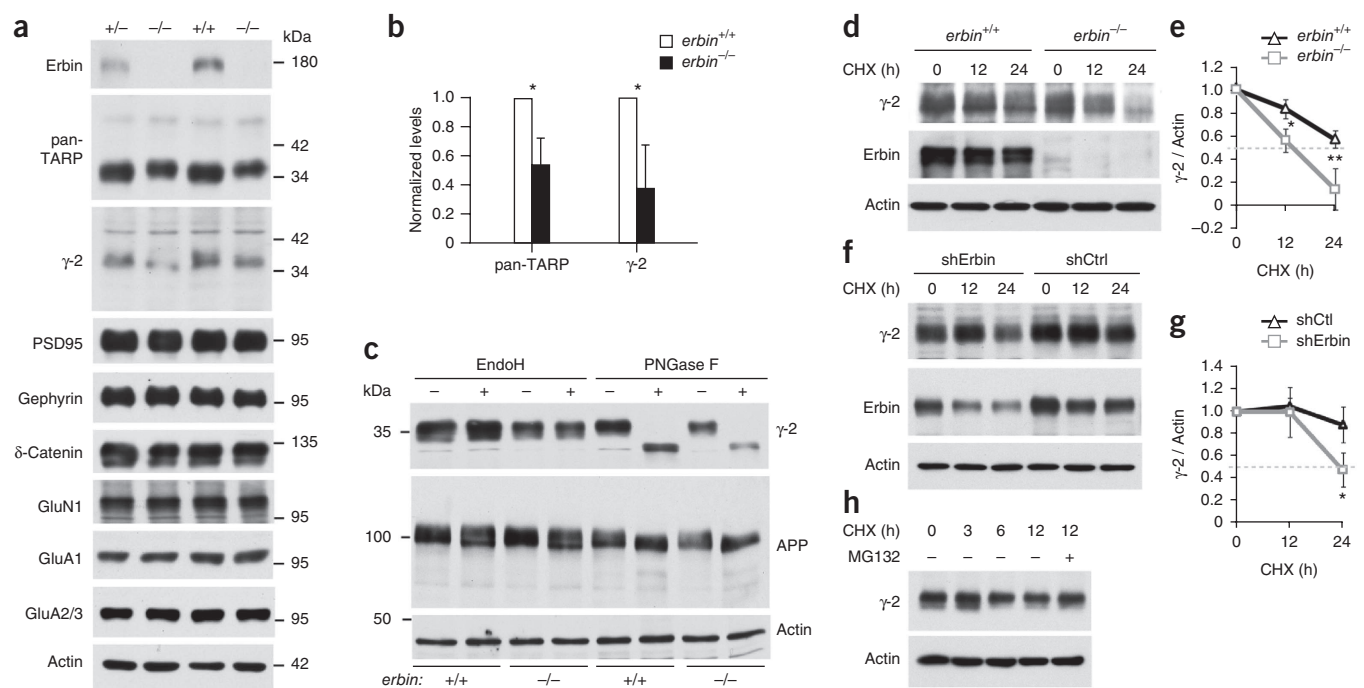


Figure 6 Stabilization of γ -2 by Erbin. (a) Reduced γ -2 levels in PSD fractions of *erbin*^{-/-} cortices. PSD fractions of indicated genotypes were subjected to western blotting with antibodies to indicated proteins. Only the 36-kDa band of TARP was reduced in *erbin*^{-/-} PSD, as compared to controls. (b) Quantitative analysis of data in a. Levels of pan-TARP (36 and 37 kDa) and γ -2 were normalized to those of actin. Error bars, mean \pm s.d., $n = 4$; $*P = 0.015$, $t = 3.896$ for pan-TARP; $*P = 0.0196$, $t = 2.629$ for γ -2; unpaired t test. (c) γ -2 in *erbin*^{-/-} brain is sensitive to PNGase F but not EndoH. P2 fractions were treated with EndoH or PNGase F, respectively, and blotted with indicated antibodies. (d) Accelerated γ -2 degradation in *erbin*^{-/-} neurons. Neurons were treated with CHX (50 μ M) for amounts of time indicated. P2 fractions were blotted with anti- γ -2 antibody. (e) Quantitative analysis of data in d. Error bars, mean \pm s.d.; $n = 4$; $*P = 0.0236$, $t = 3.260$ for 12 h; $**P = 0.0033$, $t = 4.064$ for 24 h; unpaired t test. (f) Accelerated γ -2 degradation in heterologous cells by Erbin depletion. HEK293 cells were transfected by nucleofection with control shRNA (shCtrl) or shRNA specific to Erbin (shErbin) and split evenly into six-well plates. Cells were transfected again 2 d later by Lipofectamine 2000 with γ -2. Cells were treated 24 h later with CHX (50 μ M) for amount of time indicated before lysis. Lysates were blotted with antibodies to indicated proteins. (g) Quantitative analysis of data in f. Error bars, mean \pm s.d.; $n = 3$, $*P = 0.0171$, $t = 3.162$, unpaired t test. (h) Effect of MG132 on γ -2 degradation. Neurons were treated with CHX (50 μ M) with or without MG132 (20 μ M) for amount of time indicated. P2 fractions were blotted with anti- γ -2 antibody. Full-length blots are presented in **Supplementary Figure 11**.

presence of BMI (20 μ M) and DL-AP5 (100 μ M) (**Supplementary Fig. 7c,d**), indicating no change in AMPAR intrinsic voltage dependence or polyamine affinity. Together, these data suggest that reduced synaptic transmission in PV-positive interneurons in *erbin*^{-/-} mice may occur without change in AMPAR properties.

Next, we investigated whether reduced AMPAR currents were caused by a reduction of surface AMPAR levels. Because interneurons account for only 10–20% of cortical neurons²⁸, and AMPAR is expressed in excitatory neurons as well as interneurons, it would be difficult to address this question using biochemical approaches. Therefore, we stained cortical neurons with an anti-N-terminal GluA1 antibody under nonpermeabilizing and permeabilizing conditions to assess surface and total AMPARs, respectively³⁶. PV-positive interneurons were identified by co-staining with the anti-PV antibody. GluA1 staining of nonpermeabilized PV-positive interneurons was lower in *erbin*^{-/-} mice than in wild-type controls, in intensity as well as puncta size and number, indicating a role for Erbin in regulating AMPAR surface levels (**Fig. 4a**). However, AMPAR staining was similar between permeabilized *erbin*^{-/-} and *erbin*^{+/+} PV-positive interneurons (**Fig. 4b,c**), indicating that Erbin affects only AMPAR surface expression, not total level of AMPARs. These observations are in agreement with reduced AMPAR-mEPSC amplitudes in *erbin*^{-/-} interneurons and suggest that Erbin is a previously unknown regulator of AMPAR surface expression.

Surface insertion and synaptic targeting of AMPARs may be two independent events, regulated by different mechanisms^{7,8}. The notion that Erbin regulates surface trafficking of AMPARs was corroborated by the whole-cell responses of PV-positive interneurons to brief application of the receptor agonist AMPA. Puff application of AMPA triggered transient inward currents³⁷. Ablation of Erbin decreased the amplitude of peak AMPA currents in fast-spiking interneurons (**Fig. 4d,e**), in support of the notion that surface AMPARs were reduced in *erbin*^{-/-} PV-positive interneurons.

Erbin interacts with TARP γ -2 and regulates its expression

To study mechanisms by which Erbin regulates AMPAR surface levels, we screened proteins that have been implicated in AMPAR surface expression or trafficking for their ability to interact with Erbin and identified TARP γ -2, a type I TARP that is required for AMPAR surface trafficking^{9,13,16}. TARP γ -2 co-precipitated with Erbin in transfected HEK293 cells (**Fig. 5a**), suggesting that these proteins interact in heterologous cells. To test this *in vivo*, we first determined whether TARP γ -2 and Erbin are present in same subcellular compartments of neurons. TARP γ -2 and Erbin co-purified in synaptosome and post-synaptic density (PSD) fractions of mouse cortex (**Fig. 5b**). Further, GluA1 and PSD95 were in the complex of γ -2 purified from cortical homogenates using an anti- γ -2 antibody (**Fig. 5c**), in agreement with previous reports¹³. Notably, Erbin was also present in the complex

Figure 7 Erbin regulation of γ -2 requires the γ -2-interacting domain. (a) The C-terminal region of Erbin interacts with γ -2. HEK293 cells were transfected with GFP-tagged γ -2 or γ -5 and lysed. Lysates were incubated with GST or GST-Erbin fusion proteins immobilized on glutathione-Sepharose beads. Bound proteins were subjected to western blotting with antibody to GFP. Membranes were stripped and re-probed with anti-GST antibody to indicate GST-fused Erbin proteins. IB, immunoblot; red asterisk, γ -2-GFP. (b) Summary of binding activity described in a. (c) Location of γ -2 binding activity in aa 1151–1244 of Erbin. HEK293 cells were transfected with γ -2-GFP and lysed. Pull-down assays were performed with various GST-Erbin mutant proteins as in a. After blotting, membranes were stained with Ponceau S to indicate GST-Erbin mutant proteins. (d) Summary of binding activity described in c. (e) Diagram of Erbin and Erbin₁₋₆₉₃- β -gal. (f) Reduced γ -2 levels in PSD fractions of *erbin*^{ΔC/ΔC} mice as compared to controls (*erbin*^{+/+}). (g) Quantitative analysis of results in f. Error bars, mean \pm s.d.; $n = 4$; $*P = 0.0216$, $t = 2.919$ for pan-TARP; $*P = 0.0141$, $t = 3.365$ for γ -2; unpaired t test. (h) Reduced γ -2 levels in *erbin*^{ΔC/ΔC} PV-positive interneurons. Cortical neurons (DIV17) were stained with mouse monoclonal anti- γ -2 and rabbit polyclonal anti-PV antibodies, which were visualized by Alexa 594- and Alexa 488-labeled secondary antibodies, respectively. Open arrowheads, PV-positive interneurons; solid arrowheads, PV-negative GABAergic neurons. Full-length blots are presented in **Supplementary Figure 11**.

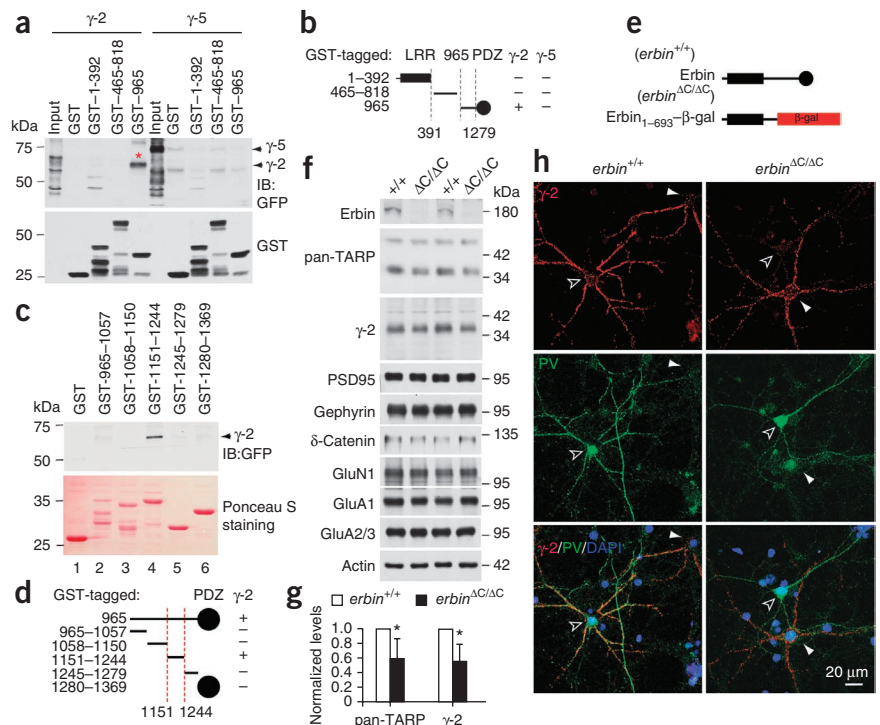


(Fig. 5c), in support of the notion that Erbin interacts with γ -2 *in vivo*. This interaction seems to be specific, because Erbin was not detectable in the complex brought down by nonspecific IgG. Moreover, ZO-1, a PDZ protein involved in interneuronal gap junctions³⁸, did not co-precipitate with γ -2 (Fig. 5c).

Having shown that Erbin interacts with TARP γ -2, we speculated that Erbin may regulate the levels or function of γ -2 and thus AMPAR surface expression. To test this hypothesis, we used a monoclonal anti- γ -2 antibody that specifically recognizes γ -2, which stained puncta in dendritic shafts of selected neurons (Fig. 5d and **Supplementary Fig. 8**). The unique staining pattern suggested that γ -2 is enriched at synapses in interneurons, which indeed were GABA-positive. To further test this idea, we stained cortical neurons with a polyclonal anti- γ -2 antibody¹² and an antibody to GAD65. The anti- γ -2 antibody labeled GAD65-positive neurons specifically (**Supplementary Fig. 8a**). These observations corroborate that γ -2 is specifically expressed in cortical interneurons, in agreement with previous reports that γ -2 mRNA levels are substantially higher in GABAergic neurons of the cortex and hippocampus^{11,12}. Quantitatively, among γ -2-expressing cortical neurons, ~60% were PV positive, whereas ~30% were SST positive (**Supplementary Fig. 8b,c**). Erbin was present in more than 93% of γ -2-positive puncta ($93.3 \pm 4.0\%$ and $94.0 \pm 5.5\%$ by the E2/E2 and 96846 antibodies, respectively) (Fig. 5e). In size and shape, Erbin-positive puncta appeared to be in better registry with γ -2-positive puncta than PSD95-positive puncta, suggesting possible extrasynaptic localization of γ -2 and Erbin.

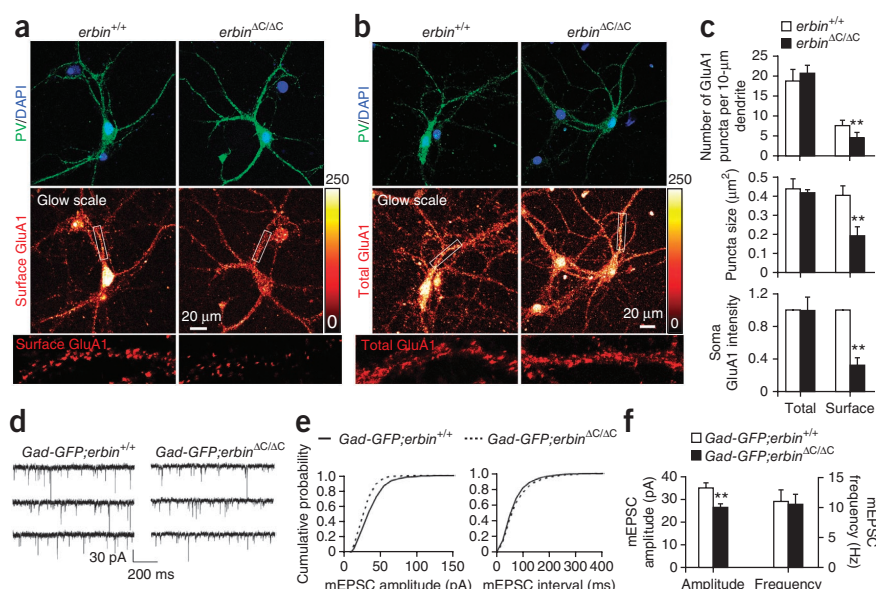
We were intrigued to find that Erbin ablation caused γ -2 reduction in PV-positive interneurons (Fig. 5f), with a PV-positive/PV-negative γ -2 intensity ratio of 1.08 ± 0.28 in *erbin*^{+/+} neurons ($n = 12$) and 0.46 ± 0.08 in *erbin*^{-/-} neurons ($n = 10$, mean \pm s.d., $P = 0.0010$, $t = 5.240$, unpaired t test), suggesting that Erbin has a function in regulating γ -2 expression. This effect was specific, as γ -2 staining in PV-negative

GABAergic interneurons was not altered by Erbin ablation (Fig. 5f and **Supplementary Fig. 8d**). Next, we determined whether γ -2 levels were reduced in PSD fractions of *erbin*^{-/-} brains. Erbin ablation had no effect on levels of PSD95, gephyrin, δ -catenin, GluN1, GluA1 or GluA2/3 in *erbin*^{-/-} mice as compared to *erbin*^{+/+} littermates (Fig. 6a). Blotting with a pan-TARP antibody, which recognizes three TARP isoforms (γ -2 at 36 kDa, γ -4 at 37 kDa and γ -8 at 45 kDa) revealed a reduction in the intensity of the 36- and 37- kDa band, but not the other bands, in PSD fractions from *erbin*^{-/-} mice (Fig. 6a). Because γ -4 is expressed mainly in glial cells^{11,12}, these results suggested a specific reduction of γ -2 in the PSD of *erbin*^{-/-} mice. We confirmed the γ -2 reduction by blotting with monoclonal or polyclonal antibodies specific to γ -2 (Fig. 6a and data not shown). Quantitative analysis indicated that the reduction of the 36- and 37-kDa band that we observed using the pan-TARP antibody was similar to that of the 36-kDa band observed using the specific anti- γ -2 antibody (Fig. 6b). These results demonstrate that γ -2 levels are reduced in *erbin*^{-/-} PSD, suggesting that Erbin is crucial for the expression of TARP γ -2 in PV-positive interneurons and that it controls AMPAR surface expression by maintaining γ -2 levels.

Involvement of Erbin in γ -2 stabilization

The reduction of γ -2 in *erbin*^{-/-} mice was unexpected. It may result from diminished transcription or a post-translational mechanism. Quantitative reverse-transcription PCR indicated that γ -2 mRNA abundance in *erbin*^{-/-} cortex is similar to that in controls, suggesting little effect of Erbin ablation on transcription of the gene encoding γ -2 or on the stability of γ -2 mRNA. To test whether γ -2 reduction is post-transcriptional, we first determined whether Erbin is necessary for the maturation of γ -2, as demarcated by N-glycosylation¹². Immature transmembrane proteins are sensitive to endoglycosidase H (EndoH)¹². Cortical membranes (P2 fractions, see Online Methods)

Figure 8 Decreased AMPAR surface expression and mEPSC amplitudes in *erbin^{ΔC/ΔC}* PV-positive interneurons. (a) Surface AMPAR levels were decreased in *erbin^{ΔC/ΔC}* PV-positive interneurons as compared to *erbin^{+/+}* neurons. DIV 17 cortical neurons were stained with anti-N-terminal GluA1 antibody under nonpermeabilizing conditions, then permeabilized and stained with anti-PV antibody. GluA1 staining intensity in primary dendrites and soma was quantified. Side bar, glow scale of GluA1 staining intensity (arbitrary unit). (b) Total AMPAR levels were not changed in *erbin^{ΔC/ΔC}* PV-positive interneurons. DIV 17 cortical neurons were permeabilized and stained with anti-N-terminal GluA1 and anti-PV antibodies. GluA1 staining intensity in primary dendrites and soma was quantified. Side bar, glow scale of GluA1 staining intensity. (c) Quantitative analysis of data in a and b. $n = 20$ cells (for *erbin^{+/+}* cultures) or 15 cells (for *erbin^{-/-}* cultures) from three independent experiments. Error bars, mean \pm s.d.; $**P = 0.0050$, $t = 3.701$ for puncta number; $**P = 0.0002$, $t = 7.360$ for puncta size; $**P = 0.0001$, $t = 12.41$ for soma GluA1 intensity; unpaired t test. (d) Representative traces of mEPSCs in fast-spiking interneurons in *erbin^{ΔC/ΔC}* mice and control littermates (*erbin^{+/+}*). (e) Cumulative distributions of mEPSC amplitudes and inter-event intervals of data in d. (f) Reduced amplitudes, but not frequencies, of mEPSCs in *erbin^{ΔC/ΔC}* PV-positive interneurons. $n = 11$ cells from six mice (both genotypes). Error bars, mean \pm s.e.m.; $**P = 0.006$, $t = 3.046$ for amplitude; $P = 0.876$, $t = 0.158$ for frequency; unpaired t test.



were subjected to EndoH treatment according to an established protocol¹². As control, membranes were also treated with PNGase F, an amidase that cleaves all N-linked carbohydrates regardless of protein maturity¹². PNGase F caused a downward shift of γ -2 from cortical membrane fractions in SDS-PAGE, demonstrating that γ -2 is N-glycosylated (Fig. 6c). However, EndoH had no effect on γ -2 in wild-type or *erbin^{-/-}* mice, although it caused a downward shift of partial β -amyloid precursor protein (APP), a transmembrane protein with multiple glycosylation states³⁹ (Fig. 6c). These observations suggest that γ -2 maturation may not be altered by Erbin ablation and that the reduced γ -2 in *erbin^{-/-}* cortex is mature.

Next, we examined whether Erbin regulates γ -2 stability. Neurons were incubated with cycloheximide (CHX), which inhibits protein synthesis, and analyzed for γ -2 expression by western blotting. γ -2 protein levels decreased faster in *erbin^{-/-}* neurons (half-life $T_{1/2} = 13.9 \pm 9.9$ h) than in controls ($T_{1/2} = 28.9 \pm 3.3$ h, $n = 4$, mean \pm s.d., $P = 0.0099$, $t = 3.751$, unpaired t test), indicating that γ -2 is unstable in *erbin^{-/-}* neurons (Fig. 6d,e). To avoid possible secondary effects caused by Erbin ablation during development, we studied γ -2 stability in HEK293 cells in which Erbin levels were acutely reduced by knock-down with small hairpin RNAs (shRNAs). γ -2 degraded faster in HEK293 cells transfected with a shRNA targeting Erbin, compared to cells transfected with control shRNA (Fig. 6f,g). These results demonstrate that Erbin is necessary for the stabilization of γ -2. In support of this notion was the observation that γ -2 reduction in cortical neurons was blocked by the proteasome inhibitor MG132 (Fig. 6h).

Interaction-dependent regulation of γ -2 stability

To investigate how Erbin regulates γ -2 stability, we mapped the Erbin domain for binding to γ -2. GST-fused Erbin (GST-Erbin) truncation mutants were purified and incubated with cell lysates from HEK293 cells transfected with γ -2. We did not detect γ -2 in precipitates by GST-Erbin₁₋₃₉₂ (GST-1-392) or GST-465-818, suggesting that the N-terminal 818 amino-acid residues are dispensable for binding to γ -2. However, γ -2 was detectable in precipitates by GST-965, a protein

containing the C-terminal region of Erbin (beginning at aa 965) (Fig. 7a,b), suggesting that the γ -2 binding region is in the C-terminal domain. GST-965 did not associate with γ -5, a type II TARP, demonstrating that Erbin interacts specifically with γ -2 (Fig. 7a,b). Further mapping with a series of GST-Erbin fusion proteins revealed that γ -2 does not interact with the PDZ domain (aa 1280-1369) but with a fragment (aa 1151-1244) preceding the PDZ domain (Fig. 7c,d). We obtained similar results in co-immunoprecipitation studies (data not shown).

We next determined whether Erbin regulation of γ -2 levels requires the domain crucial for binding to γ -2. We characterized *erbin^{ΔC/ΔC}* mice, in which *erbin* is disrupted by insertion of *lacZ* (encoding β -galactosidase (β -gal)). The *erbin^{ΔC/ΔC}* mice express an N-terminal Erbin fragment (aa 1-693) fused with β -gal (Erbin₁₋₆₉₃- β -gal)²⁷, which lacks the γ -2-interacting domain (Fig. 7e). Deletion of the C-terminal region did not affect the number and distribution of PV-positive interneurons in the cortex or their dendrite number and soma size (Supplementary Fig. 4e-h), suggesting that this mutation did not alter the development of cortical PV-positive interneurons. However, γ -2 levels were lower in cortical PSD fractions from *erbin^{ΔC/ΔC}* mice than in wild-type controls (Fig. 7f,g). The mutation did not seem to alter the levels of other synaptic proteins (Fig. 7f). Immunostaining of *erbin^{ΔC/ΔC}* cortical neurons indicated that the γ -2 immunoreactivity was reduced specifically in PV-positive, but not PV-negative, interneurons (Fig. 7h), with a PV-positive/PV-negative γ -2 intensity ratio of 1.12 ± 0.14 in *erbin^{+/+}* neurons ($n = 12$) and 0.44 ± 0.22 in *erbin^{ΔC/ΔC}* neurons ($n = 10$, mean \pm s.d., $P = 0.0012$, $t = 5.008$, unpaired t test). These results indicate that PV-positive neurons are deficient in maintaining γ -2 levels in *erbin^{ΔC/ΔC}* mice. The similarities between the *erbin^{-/-}* and *erbin^{ΔC/ΔC}* phenotypes suggest that Erbin regulates γ -2 levels by interaction.

erbin^{ΔC/ΔC} and *erbin^{-/-}* mice have similar phenotypes

To determine whether Erbin regulation of AMPAR surface expression requires the C-terminal region, we cultured cortical neurons from

control (*erbin*^{+/+}) and *erbin*^{ΔC/ΔC} mice and stained them with the anti-N-terminal GluA1 antibody under nonpermeabilizing conditions. Intensity of staining and number and size of dendritic puncta were lower in *erbin*^{ΔC/ΔC} PV-positive interneurons than in wild-type controls (Fig. 8a), indicating reduced levels of surface AMPARs. Total AMPARs in PV-positive neurons, which were characterized by staining of permeabilized cells, were similar between *erbin*^{ΔC/ΔC} mice and wild-type controls (Fig. 8b,c). This result is consistent with the notion that γ -2 regulates AMPAR trafficking from the endoplasmic reticulum to the plasma membrane rather than AMPAR synthesis. These results indicate that AMPAR surface expression in PV-positive interneurons requires the C-terminal region of Erbin. Results from electrophysiological recordings support this hypothesis. The amplitudes of AMPAR-mediated mEPSCs were lower in PV-positive interneurons of *erbin*^{ΔC/ΔC} mice than in controls (Fig. 8d–f). Deletion of the C-terminal region had no effect, however, on the frequencies of mEPSCs. Finally, although *erbin*^{ΔC/ΔC} mice had no deficits in acoustic startle response or grip strength, they were impaired in PPI and motor coordination (Supplementary Fig. 9a–d). The similarity in behavioral deficits between *erbin*^{ΔC/ΔC} and Erbin-null mice suggests that these deficits may be caused by mechanisms involving the C-terminal region of Erbin. Notably, open-field tests revealed that *erbin*^{ΔC/ΔC} mice were hypoactive (data not shown), whereas Erbin-null mice were hyperactive. This result could suggest that hyperactivity in Erbin-null mice may be caused by a mechanism that requires a different domain in Erbin.

DISCUSSION

We have identified Erbin as a previously unknown promoter of AMPAR surface expression by regulating the stability of TARP γ -2 in PV-positive interneurons. First, both Erbin and γ -2 are expressed in PV-positive interneurons and localize at excitatory synapses. Second, Erbin and γ -2 interact in a manner that requires the C-terminal region of Erbin. Third, γ -2 levels were reduced in the PSD fractions and in neurons of Erbin-null mice and *erbin*^{ΔC/ΔC} mice expressing an Erbin mutant unable to interact with γ -2. Fourth, the Erbin– γ -2 interaction is necessary for AMPAR surface levels in PV-positive interneurons. AMPAR-dependent glutamatergic transmission onto PV-positive interneurons was impaired in both *erbin*^{-/-} and *erbin*^{ΔC/ΔC} mice. Finally, *erbin*^{-/-} and *erbin*^{ΔC/ΔC} mice showed similar behavioral deficits, including impaired PPI. These observations indicate that Erbin is a γ -2-interacting protein that specifically regulates glutamate transmission onto PV-positive interneurons.

TARPs interact with various proteins, some of which contribute to AMPAR synaptic trafficking, including membrane-associated guanylate kinases such as PSD95 (refs. 13,40). AMPAR surface levels are reduced in cerebellar granule cells of heterozygous stargazer mice, but abolished in those of homozygous stargazer mice^{13,41}, indicating that regulation of AMPAR trafficking by γ -2 is dose dependent and that the maintenance of γ -2 levels is crucial. To our knowledge, Erbin is the first TARP-interacting protein found to regulate γ -2 levels in neurons. Erbin interacts with various synaptic proteins, including PSD95, δ -catenin, Cav1.3 and ErbB2 (refs. 22,23,26,42), and may form a synaptic scaffold that is necessary for γ -2 stability.

Erbin is a member of the LRR and PDZ domain (LAP) family of proteins, which contain LRRs in the N terminus and between one and four PDZ domains at the C terminus^{22,23}. Other known LAP proteins include Densin-180 in mammals⁴³, Scribble in *Drosophila*⁴⁴ and LET-413 in *Caenorhabditis elegans*⁴⁵. LAP proteins are often localized in subcellular compartments. In epithelial cells, Erbin, Scribble and LET-413 are localized at basolateral membranes and are implicated in sort-

ing proteins for polarized distribution^{22,44,45}. In neurons, Erbin and Densin-180 tightly associate with postsynaptic densities^{23,43}. Notably, Erbin is expressed specifically in PV-positive interneurons but not in pyramidal neurons. This raises the possibility that AMPAR surface expression in pyramidal neurons may be regulated by other LAP proteins, such as Densin-180.

Different types of neurons seem to be regulated by distinct TARPs⁹. We have shown here that γ -2 is specifically expressed in cortical GABAergic neurons, not pyramidal neurons. This observation is in agreement with previous *in situ* studies showing that γ -2 mRNA levels are substantially higher in cortical and hippocampal interneurons^{11,12} and imaging analyses showing that γ -2 is localized in dendritic shafts of hippocampal neurons, characteristic of excitatory synapses in interneurons⁴⁶. In PV-positive, but not PV-negative (such as SST-positive), cortical interneurons, γ -2 levels are controlled by Erbin, which is specifically present in PV-positive cortical interneurons. The observation that a reduction of γ -2 in Erbin-null mice was detectable by immunoblotting of cortical PSD fractions supports the notion that γ -2 is highly expressed in cortical PV-positive interneurons. However, Erbin was not detectable in granule cells, stellate cells or Purkinje cells in the cerebellum (Supplementary Fig. 10a–c), which may explain why mice expressing mutant Erbin did not show characteristic ‘stargazing’ phenotypes. Subcellularly, Erbin-positive puncta are in better registry with γ -2-positive puncta than with PSD95-positive puncta (Fig. 5), suggesting possible extrasynaptic localization of γ -2 and Erbin. Whether Erbin regulation of γ -2 levels occurs at synaptic or extrasynaptic sites warrants future investigation.

In addition to AMPAR surface and synaptic trafficking, TARPs, including γ -2, could modulate AMPAR channel properties, such as AMPAR gating and rectification⁹. Erbin mutation, however, seems to have no effect on the rise or decay kinetics of mEPSCs or on inward rectification of AMPAR-EPSCs. Given that TARP subunits are redundant in many types of neuron⁹, it is possible that some γ -2 functions in *erbin*^{-/-} PV-positive interneurons were compensated for by other TARPs. For example, the type II TARP γ -7 has little effect on surface trafficking of AMPARs, but it regulates their channel properties¹⁸.

Changes in glutamatergic transmission in PV-positive interneurons lead to sensorimotor gating deficits, poor working memory and social withdrawal^{31–33}. In our study, *erbin*^{-/-} mice were impaired in sensorimotor gating and motor coordination and showed reduced γ -2 levels and surface AMPARs in PV-positive interneurons, suggesting that Erbin is crucial for the regulation of AMPAR surface expression in PV-positive cells and, subsequently, of glutamatergic input. These deficits are apparently related to the Erbin interaction with γ -2, as we observed similar behavioral, biochemical and electrophysiological deficits in *erbin*^{ΔC/ΔC} mice expressing an Erbin mutant that is unable to interact with γ -2. However, *erbin*^{ΔC/ΔC} mice are hypoactive, not hyperactive as are *erbin*^{-/-} mice (data not shown), suggesting an additional function in the N-terminal region. Notably, recent evidence associates γ -2 with the pathophysiology of psychiatric disorders⁹. *CACNG2*, which encodes γ -2 in humans, resides in a region of chromosome 22 that has been implicated in schizophrenia, epilepsy and/or hearing loss⁴⁷. Genetic analysis suggests that *CACNG2* is a vulnerability gene for neuropsychologically defined subgroups of schizophrenia⁴⁸. Its aberrant expression was reported in dorsolateral prefrontal cortices of patients with schizophrenia and bipolar disorder^{49,50}. Our finding that γ -2 is enriched in cortical GABAergic neurons provides insight into the molecular mechanisms underlying the pathophysiology of psychiatric disorders.

METHODS

Methods and any associated references are available in the [online version of the paper](#).

Note: Supplementary information is available in the [online version of the paper](#).

ACKNOWLEDGMENTS

We thank S. Tomita (Yale University) and R.A. Nicoll (University of California, San Francisco) for TARP subunit constructs, Y. Yanagawa (National Institute for Physiological Sciences) for *Gad-GFP* mice, R. Haganir (John Hopkins University) for rabbit polyclonal antibodies to GluA1, GluA2/3 and GluN1, B.-S. Chen (Georgia Regents University) for the GluA1 antibody and A. Terry and K. Bouchard (Georgia Regents University) for assistance on behavioral tests. This work is supported in part by grants from VA Merit Awards and the US National Institutes of Health (NIH) (L.M. and W.-C.X.). L.M. is the Georgia Research Alliance Eminent Scholar in Neuroscience. J.-P.B. is supported by La Ligue Contre le Cancer (Label Ligue 2010). Y.T. is supported by National Nature Sciences foundation of China (NSFC 31271137). T.-M.G. is supported by NSFC 81030022, U1201225.

AUTHOR CONTRIBUTIONS

Y.T. and L.M. conceived of, designed and directed the project and wrote the manuscript; Y.T. and C.S. conducted biochemical and imaging experiments and analysis; Y.-J.C. conducted electrophysiological experiments and analysis; Y.T. and C.R.B. conducted behavioral analysis; D.L. assisted with imaging experiments and analysis; S.M. and J.-P.B. provided Erbin null mice; Z.L. and T.-M.G. assisted with data interpretation; W.-C.X. helped with data interpretation and provided instruction; L.M. supervised the project.

COMPETING FINANCIAL INTERESTS

The authors declare no competing financial interests.

Published online at <http://www.nature.com/doi/10.1038/nn.3320>.

Reprints and permissions information is available online at <http://www.nature.com/reprints/index.html>.

- Markram, H. *et al.* Interneurons of the neocortical inhibitory system. *Nat. Rev. Neurosci.* **5**, 793–807 (2004).
- Huang, Z.J., Di Cristo, G. & Ango, F. Development of GABA innervation in the cerebral and cerebellar cortices. *Nat. Rev. Neurosci.* **8**, 673–686 (2007).
- Levitt, P., Eagleson, K.L. & Powell, E.M. Regulation of neocortical interneuron development and the implications for neurodevelopmental disorders. *Trends Neurosci.* **27**, 400–406 (2004).
- Lewis, D.A., Hashimoto, T. & Volk, D.W. Cortical inhibitory neurons and schizophrenia. *Nat. Rev. Neurosci.* **6**, 312–324 (2005).
- Kawaguchi, Y. & Kubota, Y. GABAergic cell subtypes and their synaptic connections in rat frontal cortex. *Cereb. Cortex* **7**, 476–486 (1997).
- Liu, S.-Q.J. & Cull-Candy, S.G. Synaptic activity at calcium-permeable AMPA receptors induces a switch in receptor subtype. *Nature* **405**, 454–458 (2000).
- Bredt, D.S. & Nicoll, R.A. AMPA receptor trafficking at excitatory synapses. *Neuron* **40**, 361–379 (2003).
- Shepherd, J.D. & Huganir, R.L. The cell biology of synaptic plasticity: AMPA receptor trafficking. *Annu. Rev. Cell Dev. Biol.* **23**, 613–643 (2007).
- Jackson, A.C. & Nicoll, R.A. The expanding social network of ionotropic glutamate receptors: TARPs and other transmembrane auxiliary subunits. *Neuron* **70**, 178–199 (2011).
- Menuz, K., Kerchner, G.A., O'Brien, J.L. & Nicoll, R.A. Critical role for TARPs in early development despite broad functional redundancy. *Neuropharmacology* **56**, 22–29 (2009).
- Fukaya, M., Yamazaki, M., Sakimura, K. & Watanabe, M. Spatial diversity in gene expression for VDCCy subunit family in developing and adult mouse brains. *Neurosci. Res.* **53**, 376–383 (2005).
- Tomita, S. *et al.* Functional studies and distribution define a family of transmembrane AMPA receptor regulatory proteins. *J. Cell Biol.* **161**, 805–816 (2003).
- Chen, L. *et al.* Stargazin regulates synaptic targeting of AMPA receptors by two distinct mechanisms. *Nature* **408**, 936–943 (2000).
- Hashimoto, K. *et al.* Impairment of AMPA receptor function in cerebellar granule cells of ataxic mutant mouse stargazer. *J. Neurosci.* **19**, 6027–6036 (1999).
- Jackson, A.C. & Nicoll, R.A. Stargazin (TARP γ -2) is required for compartment-specific AMPA receptor trafficking and synaptic plasticity in cerebellar stellate cells. *J. Neurosci.* **31**, 3939–3952 (2011).
- Tomita, S. *et al.* Stargazin modulates AMPA receptor gating and trafficking by distinct domains. *Nature* **435**, 1052–1058 (2005).
- Menuz, K. & Nicoll, R.A. Loss of inhibitory neuron AMPA receptors contributes to ataxia and epilepsy in stargazer mice. *J. Neurosci.* **28**, 10599–10603 (2008).
- Kato, A.S. *et al.* New transmembrane AMPA receptor regulatory protein isoform, γ -7, differentially regulates AMPA receptors. *J. Neurosci.* **27**, 4969–4977 (2007).
- Soto, D. *et al.* Selective regulation of long-form calcium-permeable AMPA receptors by an atypical TARP, γ -5. *Nat. Neurosci.* **12**, 277–285 (2009).
- Fukaya, M. *et al.* Abundant distribution of TARP γ -8 in synaptic and extrasynaptic surface of hippocampal neurons and its major role in AMPA receptor expression on spines and dendrites. *Eur. J. Neurosci.* **24**, 2177–2190 (2006).
- Rouach, N. *et al.* TARP γ -8 controls hippocampal AMPA receptor number, distribution and synaptic plasticity. *Nat. Neurosci.* **8**, 1525–1533 (2005).
- Borg, J.P. *et al.* ERBIN: a basolateral PDZ protein that interacts with the mammalian ERBB2/HER2 receptor. *Nat. Cell Biol.* **2**, 407–414 (2000).
- Huang, Y.Z., Wang, Q., Xiong, W.C. & Mei, L. Erbin is a protein concentrated at postsynaptic membranes that interacts with PSD-95. *J. Biol. Chem.* **276**, 19318–19326 (2001).
- Dai, F. *et al.* Erbin inhibits transforming growth factor- β signaling through a novel Smad-interacting domain. *Mol. Cell Biol.* **27**, 6183–6194 (2007).
- Huang, Y.Z., Zang, M., Xiong, W.C., Luo, Z. & Mei, L. Erbin suppresses the MAP kinase pathway. *J. Biol. Chem.* **278**, 1108–1114 (2003).
- Laura, R.P. *et al.* The Erbin PDZ domain binds with high affinity and specificity to the carboxyl termini of δ -catenin and ARVCF. *J. Biol. Chem.* **277**, 12906–12914 (2002).
- Tao, Y. *et al.* Erbin regulates NRG1 signaling and myelination. *Proc. Natl. Acad. Sci. USA* **106**, 9477–9482 (2009).
- Tamamaki, N. *et al.* Green fluorescent protein expression and colocalization with calretinin, parvalbumin, and somatostatin in the GAD67-GFP knock-in mouse. *J. Comp. Neurol.* **467**, 60–79 (2003).
- Rudy, B., Fishell, G., Lee, S. & Hjertling-Leffler, J. Three groups of interneurons account for nearly 100% of neocortical GABAergic neurons. *Dev. Neurobiol.* **71**, 45–61 (2011).
- Gonchar, Y. & Burkhalter, A. Three distinct families of GABAergic neurons in rat visual cortex. *Cereb. Cortex* **7**, 347–358 (1997).
- Belforte, J.E. *et al.* Postnatal NMDA receptor ablation in corticolimbic interneurons confers schizophrenia-like phenotypes. *Nat. Neurosci.* **13**, 76–83 (2010).
- Fuchs, E.C. *et al.* Recruitment of parvalbumin-positive interneurons determines hippocampal function and associated behavior. *Neuron* **53**, 591–604 (2007).
- Korotkova, T., Fuchs, E.C., Ponomarenko, A., von Engelhardt, J. & Monyer, H. NMDA receptor ablation on parvalbumin-positive interneurons impairs hippocampal synchrony, spatial representations, and working memory. *Neuron* **68**, 557–569 (2010).
- Wang, H.X. & Gao, W.J. Cell type-specific development of NMDA receptors in the interneurons of rat prefrontal cortex. *Neuropsychopharmacology* **34**, 2028–2040 (2009).
- Wang, H.X. & Gao, W.J. Development of calcium-permeable AMPA receptors and their correlation with NMDA receptors in fast-spiking interneurons of rat prefrontal cortex. *J. Physiol. (Lond.)* **588**, 2823–2838 (2010).
- Beattie, E.C. *et al.* Control of synaptic strength by glial TNF α . *Science* **295**, 2282–2285 (2002).
- Milstein, A.D. & Nicoll, R.A. Regulation of AMPA receptor gating and pharmacology by TARP auxiliary subunits. *Trends Pharmacol. Sci.* **29**, 333–339 (2008).
- Li, X. *et al.* Neuronal connexin36 association with zonula occludens-1 protein (ZO-1) in mouse brain and interaction with the first PDZ domain of ZO-1. *Eur. J. Neurosci.* **19**, 2132–2146 (2004).
- Weidemann, A. *et al.* Identification, biogenesis, and localization of precursors of Alzheimer's disease A4 amyloid protein. *Cell* **57**, 115–126 (1989).
- Dakoji, S., Tomita, S., Karimzadegan, S., Nicoll, R.A. & Bredt, D.S. Interaction of transmembrane AMPA receptor regulatory proteins with multiple membrane-associated guanylate kinases. *Neuropharmacology* **45**, 849–856 (2003).
- Milstein, A.D., Zhou, W., Karimzadegan, S., Bredt, D.S. & Nicoll, R.A. TARP subtypes differentially and dose-dependently control synaptic AMPA receptor gating. *Neuron* **55**, 905–918 (2007).
- Calin-Jageman, I., Yu, K., Hall, R.A., Mei, L. & Lee, A. Erbin enhances voltage-dependent facilitation of Ca $_v$ 1.3 Ca $^{2+}$ channels through relief of an autoinhibitory domain in the Ca $_v$ 1.3 α $_1$ subunit. *J. Neurosci.* **27**, 1374–1385 (2007).
- Apperson, M.L., Moon, I.S. & Kennedy, M.B. Characterization of densin-180, a new brain-specific synaptic protein of the O-sialoglycoprotein family. *J. Neurosci.* **16**, 6839–6852 (1996).
- Bilder, D. & Perrimon, N. Localization of apical epithelial determinants by the basolateral PDZ protein Scribble. *Nature* **403**, 676–680 (2000).
- Legouis, R. *et al.* LET-413 is a basolateral protein required for the assembly of adherens junctions in *Caenorhabditis elegans*. *Nat. Cell Biol.* **2**, 415–422 (2000).
- Inamura, M. *et al.* Differential localization and regulation of stargazin-like protein, γ -8 and stargazin in the plasma membrane of hippocampal and cortical neurons. *Neurosci. Res.* **55**, 45–53 (2006).
- Knight, H.M. *et al.* Homozygosity mapping in a family presenting with schizophrenia, epilepsy and hearing impairment. *Eur. J. Hum. Genet.* **16**, 750–758 (2008).
- Liu, Y.L. *et al.* *RASD2*, *MYH9*, and *CACNG2* genes at chromosome 22q12 associated with the subgroup of schizophrenia with non-deficit in sustained attention and executive function. *Biol. Psychiatry* **64**, 789–796 (2008).
- Beneyto, M. & Meador-Woodruff, J.H. Lamina-specific abnormalities of AMPA receptor trafficking and signaling molecule transcripts in the prefrontal cortex in schizophrenia. *Synapse* **60**, 585–598 (2006).
- Silberberg, G. *et al.* Stargazin involvement with bipolar disorder and response to lithium treatment. *Pharmacogenet. Genomics* **18**, 403–412 (2008).

ONLINE METHODS

Animals. *erbin*^{-/-} and *erbin*^{ΔC/ΔC} mice were described previously²⁷. *Gad67-GFP* mice were from Y. Yanagawa²⁸. Mice (five in a cage) were housed in a room with a 12-h light/dark cycle with access to food and water *ad libitum*. Animal experiments were approved by the institutional animal care and use committee of the Georgia Regents University. Unless otherwise indicated, control mice are wild-type littermates.

Constructs, antibodies and chemicals. Mammalian expression constructs (in pRK5 and pKH3) were described previously^{23–25,51}. GST-fusion constructs were generated in pGEX2T at BamHI sites. Orientation and fidelity were verified by sequencing. TARP subunit constructs were kindly provided by S. Tomita and R.A. Nicoll^{12,41}. Rabbit Erbin antibodies E2/E2 and 96846 were generated by GST fusion with aa 465–818 and 1241–1371 of Erbin, respectively, and affinity-purified GST fusion proteins were immobilized on Affi-Gel 10 following the manufacturer's instruction. Rabbit polyclonal antibodies were gifts from R. Haganir and B.-S. Chen. Other antibodies were from Chemicon (γ -2 (cat. no. AB9876, 1:200), PSD95 (MAB1598, 1:500), GluA2 (MAB397, 1:200), GAD65/67 (AB5992, 1:200), somatostatin (MAB354, 1:200); SYSY, gephyrin (147011, 1:200), vGAT (131011, 1:200), vGluT (135311, 1:200)); Swant (parvalbumin (PV25 and PV235, 1:200)); Sigma (GAD65 (G1166, 1:200), HA (H9658, 1:2,000), myc-9E10 (M5546, 1:2,000), GABA (A2052, 1:2,000)); Santa Cruz (GluA1 (sc-13152, 1:100)); UC Davis/NIH NeuroMab Facility (pan-TARP γ -2/4/8 (clone N245/36, 1:50), γ -2 (clone N245/1, 1:50)); BD (δ -catenin (611537, 1:200), EEA1 (610457, 1:200) and Torrey Pine Biolabs (GFP (TP-401, 1:2,000)). Secondary antibodies for immunostaining (1:500) were as follows: Alexa Fluor 488 anti-mouse antibody (A11029; Invitrogen), Alexa Fluor 594 anti-rabbit (A11012; Invitrogen), and streptavidin–Alexa Fluor 594 conjugate (S11227; Invitrogen). HRP-conjugated secondary antibodies were from Amersham Biosciences. Unless otherwise indicated, all other chemicals were from Sigma.

Cell culture and transfection. HEK293 cell culture was described previously²³. Transient transfection was performed using polyethylenimine (Aldrich cat. no. 40,872-7), as described⁵². Briefly, cells were cultured in 6-well plates and at 80% confluence were incubated with precipitates formed by 4 μ g of plasmid DNA and 140 μ l of polyethylenimine 0.05% (wt/vol) for 2 h. Cells were then cultured in DMEM containing 10% FBS for 24 h before lysis.

Hippocampal and cortical neurons were cultured as described⁵³. Briefly, rodent hippocampi or cortices were dissected from E18 animals and digested in 0.25% trypsin at 37 °C for 30 min. Dissociated cells were resuspended in plating media (DMEM/F-12 50:50 supplemented with N2 and 10% FBS) and plated onto poly-L-lysine-coated 8-mm cover slips in 12 well-plates at density of 5×10^4 or 1×10^5 per well for 4 h before replacing the medium with maintenance medium (neural basal medium supplemented with B27). Half-maintenance medium was changed every 2–3 d.

Immunostaining. Brain tissues were embedded in OCT, frozen in liquid nitrogen and cut into 20- μ m sections that were mounted on SuperFrost Plus slides. Sections and cells on coverslips were fixed in 4% PB-buffered polyformaldehyde and incubated at 4 °C for 30 min with 0.3% Triton X-100 plus 5% goat serum in PBS (to permeabilize cells) then incubated at 4 °C overnight with primary antibodies in PBS containing 5% goat serum. Samples were washed with PBS then incubated at room temperature for 1 h with Alexa-488 goat anti-rabbit or Alexa-594 goat anti-mouse secondary antibody and mounted with Vectashield mounting medium (Vector). Images were taken by a Zeiss LSM510 confocal microscope. For staining of surface GluA1, neurons were fixed at 4 °C for 30 min and then blocked with 5% goat serum in PBS at 4 °C and incubated, without being permeabilized, at 4 °C for overnight with monoclonal anti-N-terminal GluA1 antibody that was visualized by Alexa-594 goat anti-mouse antibody. Images were analyzed by Image J (NIH).

Protein interaction assays. Cells were lysed in lysis buffer (50 mM Tris-HCl (pH 7.4), 150 mM NaCl, 1% NP-40, 0.5% Triton X-100, 1 mM phenylmethylsulfonyl fluoride (PMSF), 1 mM EDTA, 5 mM sodium fluoride, 2 mM sodium orthovanadate and protease inhibitors) overnight at 4 °C and centrifuged at 10,000 \times g. Resulting supernatants (cell lysate) were subjected to co-immunoprecipitation or resolved on SDS-PAGE followed by western blotting²⁷. For co-immunoprecipitation,

1 ml of lysate from transfected cells (2 mg of protein) was incubated with 1–2 μ g of antibody at 4 °C overnight and subsequently incubated with 50 μ l Protein G beads (Roche) for another hour at room temperature. Beads were washed four times with lysis buffer before the addition of SDS sample buffer.

For *in vivo* co-immunoprecipitation, mouse cortices were homogenized in buffer A (0.32 M sucrose, 1 mM MgCl₂, 1 mM PMSF and protease inhibitors) by a glass Teflon homogenizer. After centrifugation at low speed (470 \times g) for 2 min, the supernatant (S1) was mixed with equal volume of 2 \times lysis buffer (100 mM Tris-HCl (pH 7.4), 300 mM NaCl, 2% NP-40, 1% Triton X-100, 2 mM PMSF, 2 mM EDTA, 10 mM sodium fluoride, 4 mM sodium orthovanadate and protease inhibitors) and incubated overnight at 4 °C. Brain lysates were transferred into a membrane tube with a molecular weight cutoff of 7.5 kDa (Thermo Scientific) and dialyzed (1:100, vol/vol) against the dialyzing buffer (50 mM Tris-HCl (pH 7.4), 150 mM NaCl, 0.1% Triton X-100, 1 mM PMSF, 1 mM EDTA, 5 mM sodium fluoride, 2 mM sodium orthovanadate and protease inhibitors) at 4 °C overnight. Dialyzed samples were incubated with 2 μ g anti- γ -2 antibody immobilized on 50 μ l protein A beads (Roche). Resulting precipitates were resolved on SDS-PAGE and western blot with the E2/E2 anti-Erbin antibody.

GST fusion proteins were induced in BL21 cells by 100 μ M isopropyl β -D-thiogalactopyranoside and purified using glutathione-agarose beads (Roche). Beads (100 μ l, 1:1 slurry in PBS) bound with 5 μ g of GST-fused protein were incubated overnight at 4 °C on a rotating platform with one-third of cell lysates from transfected HEK293 cells in a 60-mm dish. After centrifugation, beads were washed four times with lysis buffer. Bound proteins were eluted with 2 \times SDS sample buffer and subjected to SDS-PAGE and western blotting. Resulted image was analyzed with Image J (NIH).

Postsynaptic density fraction preparation. PSD fraction of mouse cortex was prepared according to modified protocol⁵⁴. Briefly, mouse cortices were homogenized in Solution A (0.32 M sucrose, 1 mM NaHCO₃, 1 mM MgCl₂, 0.5 mM CaCl₂, 1 mM PMSF and protease inhibitors) and the homogenates were centrifuged at 470 \times g for 2 min. Resultant supernatants (S1 fraction) were centrifuged at 10,000 \times g for 10 min to obtain mitochondria- and synaptosome-enriched pellets (P2) and supernatants (S2 fraction) containing soluble proteins. P2 fractions were resuspended in 0.32 M sucrose, which was then layered onto 0.8 M sucrose. After being centrifuged at 9,100 \times g for 15 min in a swinging bucket rotor, synaptosomes (most of the loose pellets) were collected from 0.8 M sucrose layer and resuspended with equal volume of 20 mM HEPES (pH 7.0), 2% Triton X-100 and 150 mM KCl. Samples were centrifuged at 20,800 \times g for 45 min using a fixed-angle rotor, and resulting supernatants were collected as presynaptic fraction. Pellets were resuspended in a solution of 1% Triton X-100 and 75 mM KCl using a Dounce mini-homogenizer and centrifuged again at 20,800 \times g for 30 min to yield final pellets (PSD fraction), which were washed with 20 mM HEPES and dissolved in 1 \times SDS-PAGE sample buffer.

Deglycosylation assays. Endo H or PNGase F treatment was performed according to the manufacturer's manual (NEB). Briefly, P2 fractions (30 μ g of protein) of mouse cortex were denatured in 0.5% SDS with 40 mM DTT and boiled for 10 min. Denatured samples were incubated with or without Endo H or PNGase F enzymes (600 units each) for 1 h at 37 °C in respective reaction buffers. The deglycosylation reaction was stopped by addition of an equal volume of 2 \times SDS sample buffer and then boiled again for 5 min. Final products were separated by SDS-PAGE for western blotting.

Reverse-transcription quantitative PCR. Total RNA was isolated from mouse cortices using Trizol per the manufacturer's instruction (Invitrogen). Reverse-transcription quantitative PCR (RT-qPCR) was performed as described previously⁵⁵. For TARP γ -2 transcripts, primers were 5'- GAAG CTGA CACC GCAG AGTA (forward) and 5'- ATGA TGTT GTGG CGTG TCTT (reverse), which generated a product of 137 bp. Primers for internal control tubulin transcripts were 5'- ATGC GGAG AGAA ATCA TCAC CC (forward) and 5'- CCGT GGCG AACT CTTC TACG (reverse), which generated a product of 126 bp. TARP γ -2 mRNA levels were normalized to levels of tubulin assayed simultaneously on the same reaction plate.

Electrophysiology. Mice (male, 2–3 months old) with an *erbin* genotype unknown to the investigator were anesthetized with ketamine and xylazine and perfused

transcardially for 1 min with ice-cold modified artificial cerebrospinal fluid (ACSF) containing 250 mM glycerol, 2 mM KCl, 10 mM MgSO₄, 0.2 mM CaCl₂, 1.3 mM NaH₂PO₄, 26 mM NaHCO₃ and 10 mM glucose⁵⁶. Mice were decapitated and brains were quickly removed and chilled in ice-cold ACSF. Prefrontal cortical (PFC) slices (350 μm) were prepared using a Vibroslice (VT 1000S; Leica) in ice-cold ACSF. Slices were then incubated in regular ACSF containing 126 mM NaCl, 3 mM KCl, 1.25 mM NaH₂PO₄, 1.0 mM MgSO₄, 2.0 mM CaCl₂, 26 mM NaHCO₃ and 10 mM glucose for 30 min at 34 °C for recovery and then at room temperature (25 ± 1 °C) for an additional 2–8 h. All solutions were saturated with 95% O₂ and 5% CO₂ (vol/vol). Slices were placed in the recording chamber that was superfused (3 ml per minute) with ACSF at 32 °C. Whole-cell patch-clamp recording of layers II–V neurons was aided with infrared optics using an upright microscope equipped with a ×40 water-immersion lens (BX51WI, Olympus) and an infrared-sensitive charge-coupled device (CCD) camera.

To record action potentials, pipettes (input resistance, 4–6 MΩ) were filled with the intracellular solution containing 105 mM K-gluconate, 30 mM KCl, 10 mM HEPES, 10 mM phosphocreatine, 4 mM ATP-Mg, 0.3 mM GTP-Na and 0.3 mM EGTA (pH 7.35, 285 mOsm). To characterize membrane and firing properties of interneurons, hyperpolarizing and depolarizing current steps were applied for 200 ms at 0.2 Hz in current-clamp configuration. Biocytin (0.2%) was added to the pipette solution to identify recorded neurons by immunostaining with anti-PV antibody. To record mEPSCs, GABA_A receptor and action potentials were blocked with 20 μM BMI and 1 μM TTX, respectively. For NMDAR-mediated mEPSCs, CaCl₂ and MgSO₄ in ACSF were replaced by 3 mM SrCl₂ in the presence of 20 μM CNQX to inhibit AMPAR-mediated currents. For local application of AMPA, a puff pipette with a tip resistance of 4–5 MΩ was filled with 500 μM AMPA (Tocris, in ACSF) and placed about 20 μm away from recorded cells. Positive pressure was applied (6 p.s.i., 5–30 ms) at intervals of 120 s using a Pressure System Ite (Toohey Company). AMPA-evoked currents were recorded at a holding potential of –70 mV in the presence of 100 μM DL-AP5, 20 μM BMI and 0.5 μM TTX (to silence the network).

AMPA-EPSCs, which can be inhibited by CNQX (20 μM), were evoked with a two-concentric bipolar stimulating electrode (FHC) placed 300 μm away from recorded neurons at –70 mV in the presence of BMI (20 μM) and DL-AP5 (100 μM). To record action potentials and EPSCs with minimal K⁺ currents, the whole-cell recording pipette were first filled with a K⁺-gluconate-based intracellular solution at the tips and then back-filled with Cs⁺-containing solution of 135 mM Cs-methanesulfonate, 8 mM NaCl, 10 mM HEPES, 10 mM phosphocreatine, 4 mM ATP-Mg, 0.3 mM GTP-Na, 0.3 mM EGTA and 5 mM QX314 (pH 7.3, 290 mOsm)³⁴. Paired-pulse ratio of EPSCs in fast-spiking interneurons was measured in response to stimulations at 50-ms intervals. To characterize I–V curves, AMPAR-EPSCs were recorded with pipettes filled with intracellular solution containing 100 μM spermine at holding potentials of –60 mV to +40 mV, in 20-mV steps. The rectification index (RI) was determined by the

following formula: $RI = (I_{+40} / I_{-60}) \times [(-60 - E_{rev}) / (40 - E_{rev})]$, where I₊₄₀ and I₋₆₀ are peak amplitudes of the EPSCs holding steadily at +40 mV and –60 mV, respectively, and E_{rev} is reversal potential. To record mIPSCs, CsCH₃SO₃ and NaCl were omitted; the concentration of CsCl was increased to 140 mM to enhance the driving force of Cl⁻, and 20 μM CNQX, 100 μM DL-AP5 and 1 μM TTX were added in the bath solution. The data were recorded with a MultiClamp 700B (Molecular Devices), digitized at 10 kHz and filtered at 1 kHz. Data were collected when series resistance fluctuated within 20% of initial values and analyzed by pClamp 9.2 software (Molecular Devices).

Behavioral analysis. Behavioral tests were carried out in the morning with 12- to 16-week-old mice (60% male, 40% female in each group except for tests (PPI) in which only males were used) by investigators unaware of the mice's genotypes in the Small Animal Behavior Core Facility of Georgia Regents University. Open-field and PPI tests were described before⁵⁷. To evaluate sensorimotor coordination, mice were placed on an accelerating rotarod (Rotor-Rod System, San Diego Instruments) and assessed for ability to maintain balance on the rotating bar that accelerated from 4 to 40 r.p.m. over a 5-min period. Mouse latency before falling from the rod was recorded. To evaluate a mouse's motor function and muscle strength, we placed its forelimbs on a tension bar and pulled the mouse back gently until it released the bar. Grip strength was determined by a digital grip-strength meter (Animal Grip Strength System, San Diego Instruments). Mice were tested for open field and then for PPI, rotarod and grip strength, with a 1-week break after each test.

Statistical analyses. Data were analyzed by Student's *t* test and ANOVA. *P* < 0.05 was considered statistically significant.

51. Yang, X.L., Huang, Y.Z., Xiong, W.C. & Mei, L. Neuregulin-induced expression of the acetylcholine receptor requires endocytosis of ErbB receptors. *Mol. Cell Neurosci.* **28**, 335–346 (2005).
52. Simeone, L. *et al.* Identification of Erbin interlinking MuSK and ErbB2 and its impact on acetylcholine receptor aggregation at the neuromuscular junction. *J. Neurosci.* **30**, 6620–6634 (2010).
53. Huang, Y.Z. *et al.* Regulation of neuregulin signaling by PSD-95 interacting with ErbB4 at CNS synapses. *Neuron* **26**, 443–455 (2000).
54. Dosemeci, A., Tao-Cheng, J.H., Vinade, L. & Jaffe, H. Preparation of postsynaptic density fraction from hippocampal slices and proteomic analysis. *Biochem. Biophys. Res. Commun.* **339**, 687–694 (2006).
55. Liu, X. *et al.* Specific regulation of NRG1 isoform expression by neuronal activity. *J. Neurosci.* **31**, 8491–8501 (2011).
56. Thomson, A.M., West, D.C., Hahn, J. & Deuchars, J. Single axon IPSPs elicited in pyramidal cells by three classes of interneurons in slices of rat neocortex. *J. Physiol. (Lond.)* **496**, 81–102 (1996).
57. Wen, L. *et al.* Neuregulin 1 regulates pyramidal neuron activity via ErbB4 in parvalbumin-positive interneurons. *Proc. Natl. Acad. Sci. USA* **107**, 1211–1216 (2010).

Corrigendum: Erbin interacts with TARP γ -2 for surface expression of AMPA receptors in cortical interneurons

Yanmei Tao, Yong-Jun Chen, Chengyong Shen, Zhengyi Luo, C Ryan Bates, Daehoon Lee, Sylvie Marchetto, Tian-Ming Gao, Jean-Paul Borg, Wen-Cheng Xiong & Lin Mei

Nat. Neurosci. 16, 290–299 (2013); published online 27 January 2013; corrected after print 30 July 2013

In the version of this article initially published, the email address for correspondence was given as lmei@grc.edu. The correct address is lmei@gru.edu. The error has been corrected in the HTML and PDF versions of the article.